Evaluation of Received Dose Distribution of ^{18}F Production with Iranian Sun Plasma Focus Device (IS)

H. Rokhzadi-zardouei [1], M. Hasanzadeh[*2], A.Refaee[3], and S. M. Sadat-Kiai[4]

[1,3]Department of physics, Sanandaj Branch, Islamic Azad University, Sanandaj, Iran

[2]Reactor and Nuclear Safety Research School, Nuclear Science and Technology Research Institute (NSTRI), AEOI, Tehran, Iran

[4]Plasma and Nuclear Fusion Research School, Nuclear Science and Technology Research Institute (NSTRI), AEOI, Tehran, Iran

* Corresponding Author

Abstract

The best way to use radioisotopes with short half-lives is to produce them at the injection site.

Iranian Sun Plasma focus Device is a nuclear fusion reactor that is convenient for radioisotopes produced with short half-lives for medical use. Here have been used same geometries with IS device. In this Theoretical study, H_2O and O_2 targets were used for ^{18}F production. This study compared the dose and energy distribution, in water and G4_MUSCLESKELETAL_ICRP phantoms at different distances and directions from the proton source. The beam-target mechanism was simulated by the GEANT4.10.7 tool and used the G4EmStandard Physics_option3 physic model. To provide a more accurate simulation of particle ranges in physics constructors for the 18F production with the 10^7 protons in each shake with 5.02 MeV energy, of course, to get this energy, there is a need to review the structure of this device. Dose distributions in the vertical direction are half of Dose distributions in the same direction of the source beam. The dose profile for G4_MUSCLESKELETAL_ICRP and H2O phantoms match 99% obtained by gamma index matching.

Keywords: Geant4.10.7, ^{18}F production, Iranian Sun plasma focus, Scan Dose Match, Dose distribution

Tob Regul Sci.™ 2022;8(2): 187-195
DOI: Doi.Org/10.18001/TRS.8.2.11

1. Introduction

1.1 ^{18}F radioisotope production

The best way to use radioisotopes with short half-lives is to produce them at the injection site. It found that the plasma focus device is suitable for producing PET radioisotopes. ^{18}F has a half-life of about 110 minutes, it has the most widely used and desirable radioisotope in the PET method, and processing tools have become very important. The importance of 18F has two parts of

production and Medical use.^{18}F is a great radioisotope in radiotherapy. This positron-emitting radioisotope has a substantial role in the imaging by positron pet emission. In this study, to produce 18F with the knowledge of dose receiving standards, Doses that reached two phantoms and directions have been evaluated.

According to Table1. H_2O and O_2 collision with 5.02 MeV proton beams have been selected for ^{18}F producing [1, 2, 3].

Table 1. The most important reactions of ^{18}F radioisotope production

Equation	Threshold energy (MeV)	Cross section (mb)	Target
$^{18}O(p,n)^{18}F$	5.02	585.9	$^{18}O_2$, H_2O
$^{20}Ne(d,\alpha)^{18}F$	6.1	222.4	^{20}Ne, Ne / F_2
$^{16}O(^3He,p)^{18}F$	6.35	436.0	H_2O

1.2 Plasma focus device

A plasma focus device is a device that can produce hot and dense plasma with a short life of about 50 ns using electromagnetic compression and acceleration.

The device includes an anode and a cathode, which are separated by a special insulator that causes a breakdown during the discharge of the capacitors. There are two types of Iranian sun Dense Plasma Focus (DPF)[1], Filippov, and Mather. The vacuum chamber, turnover of spark cap, and capacitor banks are the main components and the power supply, vacuum system, diagnostic tools, and automated data processing systems are the subdivisions part of the device. We have depicted a schematic of IS DPF (Fig.1). [4, 5, 6, 7, 8,]

Different gas fuels are used for various proposes at different pressures in a plasma focus device including helium, neon, argon, xenon, nitogen, deuterium, et. We use only deuterium (D) gas fuel to generat the following reaction plus reaction plusreaction$+D \rightarrow {}^{3}H_e + n(2.45\ MeV)\ \ D + D \rightarrow T + +T \rightarrow {}^{4}H_e + (14.1\ MeV)$

$^{3}H_e + D \rightarrow {}^{4}H_e + (14.66\ MeV)$

Reports show that by changing the energy of the capacitive bank from 1 kJ to 1 MJ, the particle emission changes from 10^7 to 10^{12} particles per pulse. While this amount of radiation and its types are enough for experiments, this radiation poses have a risk of radiation to device operators. Decreasing the radiation dose getting by operators will not be achieved without placing the device in a remote place. [9, 10, 11, 12, 13, 14]

[1] Dense plasma focus

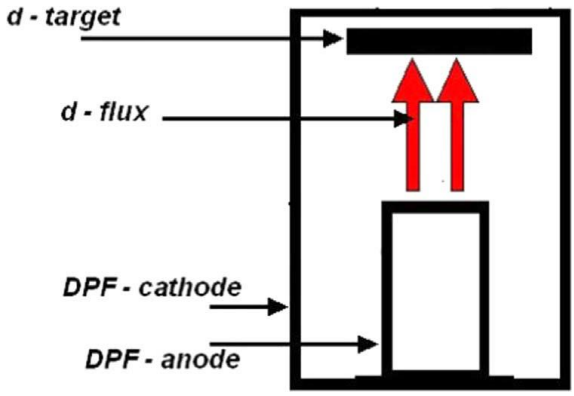

Fig. 1 The simplified geometry of the DPF system and the two beam-target mechanisms.

Research by the IS DPF has been on neutron production and irradiation, and this study with the proton beams is theoretical.

2. Material and Method

Many experimentally and theoretically researches have been done using the beam-target mechanism to produce Short Life Radioisotopes (SLRs) [7-9]. Here, we use IS DPF device as an accelerator with GEANT 4 toolkit [10, 11, 12, 13, and 14].

This study was stimulated by Geant 4.10.7. This Simulation has done with real geometry of IS DPF has been shown in Fig.2. Also, Iranian Sun plasma focus device bases to simulate have shown in Tables.2, 3 [15, 17, 18, 19].

Fig. 2 Iranian Sun plasma focus device

Table 2. The structures used to simulate the Iranian Sun plasma focus device

Cell	Material	Thickness(cm)	Density (g/cm^3)
Reflector	Pb	2	11.34
Collimator	Pb	9	11.34
Filter	Bi	3	9.78
Moderator	Al	2	0.669

Table 3. The operational and geometrical parameters of IS DPF.

Specific heat ratio of the deuterium γ	$\frac{5}{3}$
Deuterum in mass m_d	10^{-27} kg010^{-27} kg
Tritium on mass m_t	
DThe densityof deuterium ρ_d	10^{-3} $\frac{kg}{m^3}$
The permittivitof free space ε_0	$8.854 \times 10^{-12}(\frac{F}{m})$
Electric charge e	1.602×10^{-19} (C)
PThe pressureyof D gas	10orr
pedane $Z_0 = \sqrt{\frac{L_0}{C_0}}$	$Z = 12.5$ mΩ
$= I_0 \approx \frac{V_0}{\sqrt{\frac{L_0}{C_0}}}$	$I_0 = 433445$
Maximum harng voltage V_0	$V_0 = 30$ kV
itor bank C_0	$C = \mu F$
Stored bank energy E	15J
The inductance of the circuit L_0	160×10^{-9} H
Period of circuit trace T_0	$t_0 = 2\pi\sqrt{L_0 C} = 3.6$ μs
The dose Anode radius a	1.5m
Anode length Z_0	15 cm
Cathode radius b	5.25m
Axial speed V_a	$\times 10^4$ $\frac{m}{s}$
Radial speed V_r	1.110^5 $\frac{m}{s}$
Pinch radius r_p	1.8m
Pinch lifetime τ_p	The 30s
Pinch length d	.2
$c = \frac{b}{a}$ 3.5	
Current loss factor	0.6
Mas-swep fctor f_m	0.2
Induced voltage ϕ	8.110^4 V

distribution received to water phantom cube with dimensions of 20 cm at two distances of 70 cm and 20 cm from source for 18F producing has been used the 107 protons with 5.02 MeV energy to collision with H2O and O2 targets in each shut [20, 21, 22]. Figure 3 shows the simulation of the Iranian Sun plasma focus device geometry with the Geant 4.10.7 tool.

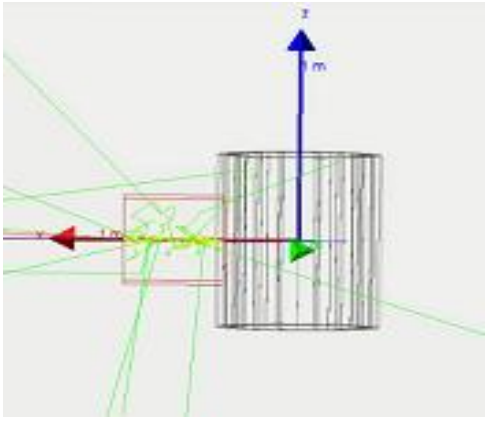

Fig. 3 Simulation of the Iranian Sun plasma focus device geometry with Geant 4.10.7 code

3. Results and Discussion

3.1 Calculation of dose distribution

In this study, dose and energy distribution in terms of distance indicated dose and energy distributions of particles that leave the device.

Figure 4 shows dose distributions for H2O and O2 targets at the center of the device, the maximum dose is 30.4 μGy, in 30 cm from the source, the dose reduced in the 42 cm from H2O and 44 cm from O2 targets.

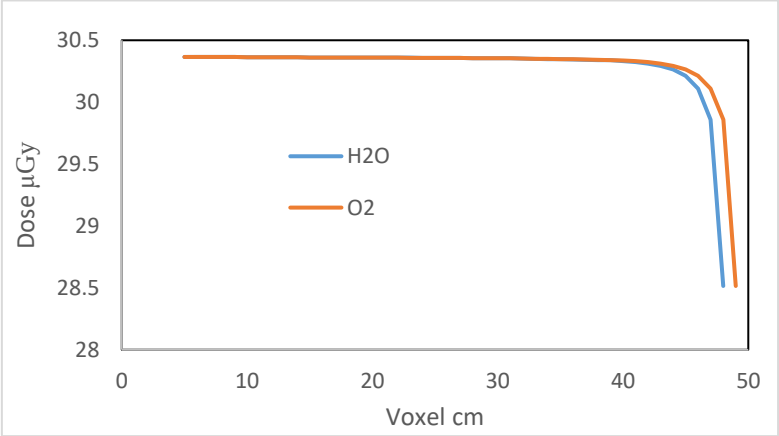

Fig. 4 Dose distribution at 20 cm from source of the device for H_2O and O_2 targets

Figure.5 shows the dose distribution for G4_MUSCLESKELETAL_ICRP (from H2O target) and G4_MUSCLESKELETAL_ICRP (from O2 target) phantoms. Max dose distribution is the same 30.4 μGy. For the H2O Phantom, dose distribution in 24 cm from the device, and 74 cm from the proton Source, has been zero.

For the G4_MUSCLESKELETAL_ICRP phantoms, dose distribution, has been zero in 23 cm from the device, and 73 cm from the proton source.

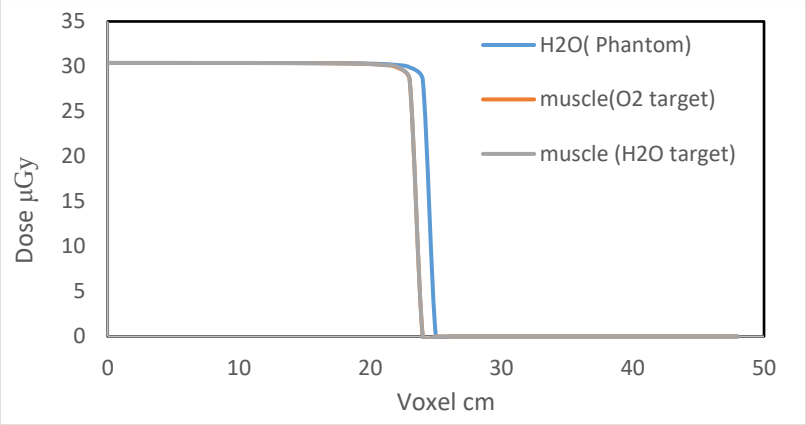

Fig. 5 Dose distribution outer the device for H_2O phantom, G4_MUSCLESKELETAL_ICRP (H_2O target), and muscle (O_2 target) Phantom

Figure.6, shows, that the dose distribution is zero in the vertical direction at 23 cm from the device. Dose distribution on the Vertical side of the source beam has been half of the max dose distribution on the same side on the source beam and almost constant in the G4_MUSCLESKELETAL_ICRP phantom.

Dose distribution has been zero for the same direction with the source beam at 23 cm out of the device. Dose distribution in the vertical side on the source beam has been half of the max dose distribution in the same direction on the source beam and almost constant.

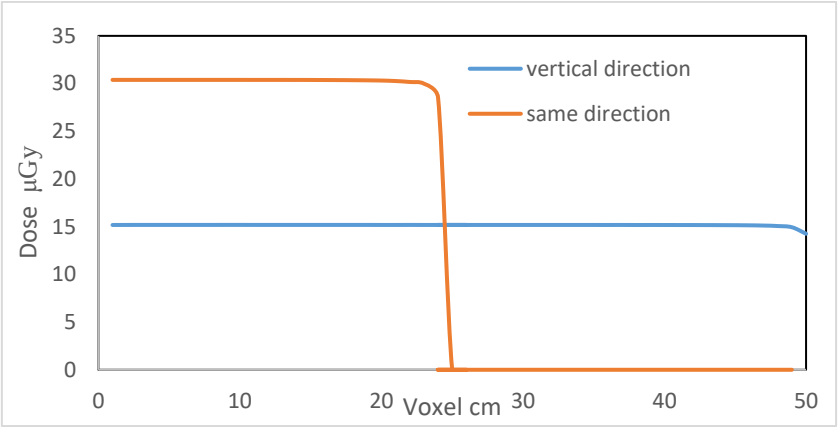

Fig. 6 Dose distribution of Vertical and same direction with beam proton in G4_MUSCLESKELETAL_ICRP phantom

3.2 Total energy

The total energy is the sum of all of the secondary particle's energy.

Fig.7 shows the range of the log total energy deposited is the same, for H2O and muscle phantom about 10 – 1000000 MeV.

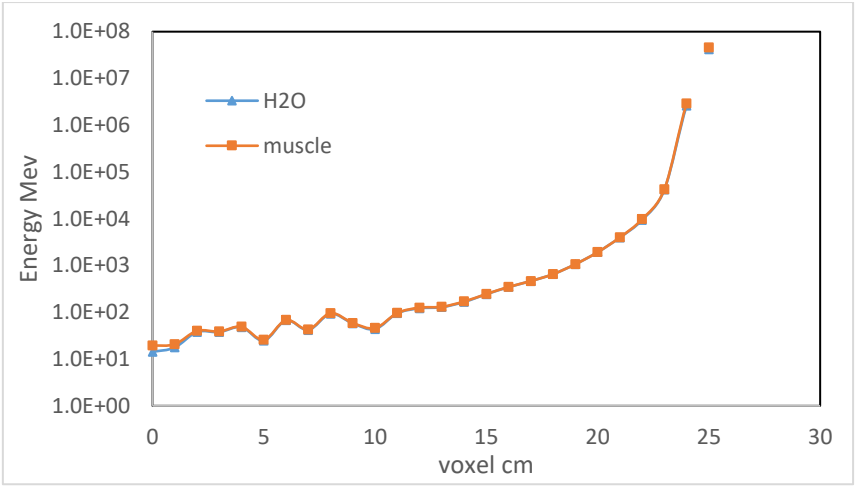

Fig. 7 Log total energy in H_2O and G4_MUSCLESKELETAL_ICRP phantom

In Fig. 8, the total energy increase when secondary particles create. As the distance from the source increases, the total energy becomes zero. Because of the wide range of energy quantity, the difference in the two phantoms is hardly visible.

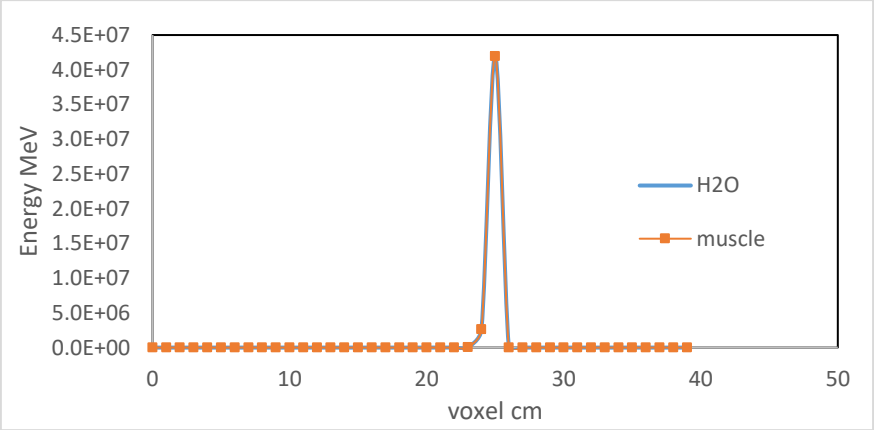

Fig. 8 Phantom total energy for H_2O and G4_MUSCLESKELETAL_ICRP phantom

4. Conclusions

The gamma index in the scan Dose Match program is a coefficient for the quantity of difference in the reference and measured profile results. The gamma index, for values less than or equal to 1, is acceptable.

For the unavailability of experienced results by this device, comparing the results with two different phantoms is used. For the reference profile column data, the results of the water phantom, and for the measured profile column data, the results of G4_MUSCLESKELETAL_ICRP have been set. In Fig. 9 and 10, the gamma index is equal to and less than one, which indicates a 99% matching. Skeletal muscle is composed of 70% water, 20% protein, and 5% carbohydrates then this tissue has an almost similar density to water, so the results of both phantoms are compatible.

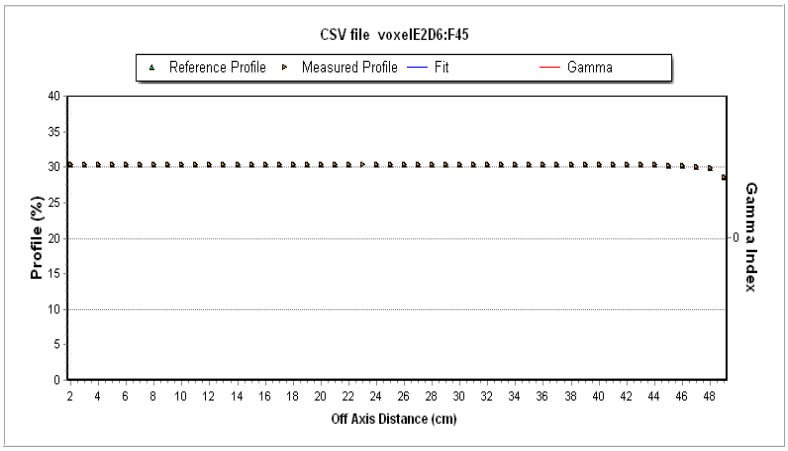

Fig. 9 Dose matching simulation result H2O target in the G4_MUSCLESKELETAL_ICRP and water phantoms on 20cm from beam source

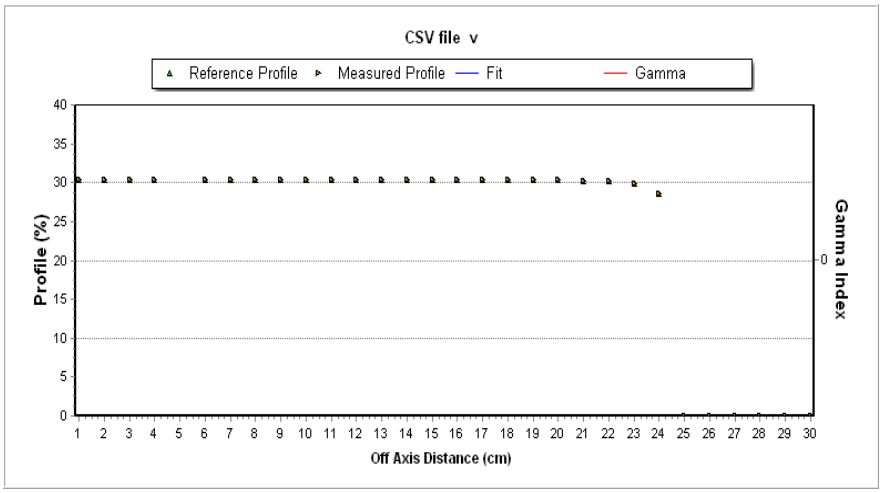

Fig. 10 Dose matching simulation result for H_2O target in the G4_MUSCLESKELETAL_ICRP and water phantom on 50cm from beam source

In real experiment experiences, according to these results for operating, radiation minimized by holding a distance of about 25 cm from IS DPF for operators.

References

1. M. Ravanelli et al. Value of [18F] FDG PET-CT in the follow-up of surgically treated oral tongue squamous cell carcinoma: single center cohort analysis on 87 patients, Nuclear Medicine Review 2021, 24, 2: 58–62.
2. A. Fathala et al. Patterns of [18F] FDG myocardial uptake in oncology patients as a predictor of myocardial is chemical on stress myocardial perfusion imaging, Nuclear Medicine Review 2021, 24, 2: 51–57.
3. Maciej Kolodziej, Evaluation of the usefulness of positron emission tomography with ^{18}F fluorodeoxy lglucose performed to detect non-radioiodine avid recurrence and/or metastasis of differentiated thyroid cancer a preliminary study, Nuclear Medicine Review , 2021;24(2):63-69.

4. Roshan, M.V., Springham, S.V., Rawat, R.S., Lee, P., 2010. IEEE Trans. Plasma Sci. 38 (12), 3393–3397.
5. Roshan, M.V., et al., 2014. Phys. Lett. A 378, 2168–2170.
6. Saed, M., Roshan, M.V., Banoushi, A., Habibi, M., 2016. J. Mod. Phys. 7, 1512–1518.
7. Talaei, A., kiai, S.M., Zaeem, A.A., 2010. Appl. Radiat. Isot. 68 (12), 2218–2222.
8. S. GB., Radioactive decay and interaction of radiation with matter, basics of pet imaging. Cham: Springer; 2016.
9. EL. Cole, MN. Stewart, R. Littich, et al. Radio syntheses using fluorine-18: the art and science of late stage fluorination. Curr Top Med Chem 2014; 14(7):875–900.
10. F. Castillo et al. Evidence of Thermal and Non-Thermal Mechanisms Coexisting in Dense Plasma Focus D-D Nuclear Reactions J. Phys, D: Appl. Phys. 33 (2000) 141-147.
11. Geant4 Collaboration, Introduction to GEANT4 User Documentation (2009).
12. K. Hubner et al. Fusion Reaction Rate for A Plasma Boiler Moving an Ambient Plasma, Volume 69A, No 4, Physics Letters Dec. 1978.
13. A. Serban et al. Correlation of Neutron Anisotropy with Neutron Yield and Soft X-ray Production from a Plasma Focus, 27th EPS Conference on Contr. Fusion and Plasma Phys. Budapest, 12-16 June 2000 ECA Vol. 24B (2000) 1677-1680s.
14. S. M. Sadat Kiai, design a 10KJ is mather type Plasma Focus for solid target activation to produce short-lived Radioisotopes ^{12}C (d,n)^{13}N, Fusion Energy. Volume29, (2010), 421-426.
15. A. Talaei et al, Interaction of the high energy deuterons with the graphite target in the plasma focus devices based on lee model, Appl. Rad. Isotopes, volume 68,(2010) 2218-2222.
16. F. Ditroi, et al., Gas, Liquid and Molten Targets at Cyclotron Beams: Target Systems and Related Nuclear Database, (2009).
17. J. Allison, et al., Geant4 developments and applications, IEEE Nucl. Plasma, volume (53), (2006), 270-278.
18. M. Nanbedeh, et al., A feasibility study of the Iranian Sun Mather type plasma focus source for neutron capture therapy using MCNPX2. 6, Geant4 and FLUKA codes, Nuclear Engineering and Technology, volume 25, (2019).
19. M. Clemencic, et al. The LHCB simulation application, Gauss: design, evolution and experience, Journal of Physics: Conference Series. Vol. 331. No. 3. IOP Publishing (2011).
20. M. AKel, et al., Interaction of the high energy deuterons with the graphite target in the plasma focus devices based on Lee model, phys. Physics of Plasmas, volume 21, (2014), 072507-1.
21. S. Lee and S. H. Saw, Plasma focus ion beam flounce and flux—Scaling with stored energy, volume (19), (2012), 112703 (1-5).
22. P. Rowshanfarzad, et al. An overview of copper radionuclides and production of Cu-61 by proton irradiation of Zn-nat at a medical cyclotron, Vol 64(12), 2007, 1563-73.
23. Physics Reference Manual Version: geant4 10.7(5 December 2014).